IRANIAN JOURNAL OF CATALYSIS

Non-noble supported catalyst for oxidation of glucose under mild reaction conditions

Mohd Hasbi Ab. Rahim[a,b]*, Ng Pui Xin[a], Anisah Sajidah Haji Saud[a], Mohd Asyrak Deraman[a], Gaanty Pragas Maniam[a, b, c]

a) Department of Industrial Chemistry, Faculty of Industrial Sciences and Technology, University Malaysia Pahang, Lebuhraya Tun Razak, Gambang, 26300, Pahang, Malaysia
b) Earth Resources & Sustainability Centre, University Malaysia Pahang, Lebuhraya Tun Razak, Gambang, 26300, Pahang, Malaysia
c) Central Laboratory, University Malaysia Pahang, Lebuhraya Tun Razak, 26300 Kuantan, Pahang, Malaysia

Received 25 April 2020; received in revised form 1 December 2020; accepted 7 February 2021

ABSTRACT

Catalytic oxidation of D-glucose to D-gluconic acid derivative with H_2O_2 has been studied using non-noble Cobalt supported catalyst. The catalysts were synthesized using the scalable incipient wetness impregnation method of Co/Al_2O_3 and Co/TS1. The catalysts have been characterized by TGA, XRD, FESEM-EDX, BET, FTIR, and Hammett test. The oxidation of the D-glucose into D-gluconic acid with yield of 82% (as sodium gluconate) and selectivity is about 100 % have been achieved in the presence of 5 wt.% Co/Al_2O_3 as a catalyst under mild reaction conditions (60 °C, pH 9, 1atm, 3h). Reusability study of Co/Al_2O_3 was proven to be stable for subsequent cycles of reaction with no notable changes in selectivity. Besides, the physic-chemical properties of spent catalyst were similarly characterized through FTIR and Hammett test analysis. The presence of gluconic acid was confirmed by HPLC. The apparent activation energy of reaction is 15 kJ mol^{-1} which is lower than the value reported by prior-art using gold catalysts suggesting different mechanism with dissimilar rate-determining step. The activation of H_2O_2 is mediated by Co crystallites on the catalyst surfaces, forming active oxygen species via hydroxyl and peroxyl radical intermediates and/or oxometal species. The basic sites on catalyst facilitate the activation of glucose. The findings could help to make a cost-effective catalyst for D-glucose conversion into valuable organic acid chemical.

***Keywords**: Cobalt supported catalyst, Non-Noble Metal, D-Glucose oxidation, D-Gluconic acid, Sodium Gluconate*

1. Introduction

Glucose ($C_6H_{12}O_6$) is one of the essential carbohydrate feedstocks to produce industrial chemicals. Generally, it can be converted into a broad range of products through isomerization, dehydration, hydrogenation and selective oxidation reactions, either via biochemical or chemical processes [1-3]. One of the important and valuable chemicals derived from glucose as a starting feedstock is gluconic acid ($C_6H_{12}O$). The world market of gluconic acid is standing at $ 51.6 billion in 2018 and is expected to grow further due to its wide applications [4].The gluconic acid and its derivatives (i.e. its salts and gluconolactones) are used in various fields of industry especially in food, pharmaceuticals and chemical industries are one of the key drivers for gluconic acid market [5].

In the past decade, the ability of hydrogen peroxide, H_2O_2, to promote high catalytic activities under atmospheric pressure has stimulated the interest towards the use of H_2O_2 as an environmentally friendly oxidant for glucose oxidation at large scale. Ishida et al. [6] studied the oxidation of D-glucose with H_2O_2 on Au catalysts supported with diverse polymers. Primarily, not more than 50% of D-glucose conversions are observed by relating 1.6 equiv. of H_2O_2 to D-glucose. They pointed out that D-glucose oxidation is probably facilitated with the intermediate oxygen species formed via H_2O_2 decomposition. A similar claim on the active species was reported by Saliger et al. [7] in the presence

*Corresponding author:
E-mail address: *mohdhasbi@ump.edu.my* (M. H. Ab Rahim);

of a highly active Au/Al_2O_3 catalyst. The reactions are carried out under alkaline conditions mainly to assist the reaction mechanism through deprotonation of hydroxyl group and rendering C-H rate-limiting. Also, the formation of gluconate salt reduces the catalyst poisoning due to inhibition effect of acid product [8, 9]. Indeed, gluconate product makes up about 80% of the gluconic acid market [10].

As the preferred commercialized biochemical route faced recyclability and product contamination issues whereas conventional chemical approach releases toxic and hazardous materials to the environment, many researchers have put much attention towards catalytic oxidation of glucose to gluconic acid with the use of selective heterogeneous catalyst, especially noble metal catalytic systems. Nevertheless, the development of selective chemo-catalytic routes for large scale production of gluconic acid from glucose remained challenging and yet to be commercialized, which is mainly associated with technological, practical, environmental challenges, as well design of a robust and active catalyst [11, 12]. The model catalytic system for glucose oxidation is a precious metal by means of platinum, palladium, rhodium and gold, with either one support of carbonaceous materials, metal oxides, layered double hydroxide, and polymer or cellulose [6, 7, 13-19]. Utilization of a precious metal will eventually increase the overall cost of production. Therefore, it is crucial to find alternative cheaper metal catalysts with comparable or higher catalytic yield.

In the present work, the concern about environmental protection increases over the years from a global viewpoint and the cost of the process the selective catalytic oxidation of D-glucose with H_2O_2 using cobalt supported catalysts is reported. The aims of this work are to study and compare the catalytic performance of Co/Al_2O_3 and Co/TS-1 catalysts which are reusable, environmentally friendly, and low cost. An investigation on the optimum reaction conditions with regards to the influence of temperature, pH, glucose concentration and amounts of H_2O_2 on catalyst activity, conversion, selectivity and stability were also carried out to find the better catalytic system, in addition to the mechanistic of heterogeneous catalyst.

2. Experimental

2.1. Catalysts Preparation

Alumina (γ-Al_2O_3) purchased from Sigma Aldrich and Titanium Silicate-1 (TS-1) supplied by Advance Chemical Supplier (ACS) materials were used as support material. The AR grade Cobalt (II) Nitrate hexahydrate ($Co(NO_3)_2\cdot 6H_2O$ ≥99.0%) used as cobalt precursor, and AR grade D-glucose and 30 wt.% H_2O_2 used for catalytic oxidation were all purchased from Sigma Aldrich. These chemicals were used without further purification. Deionized water was used throughout this work.

The 5 wt.% Co/γ-Al_2O_3 and 5 wt.% Co/TS-1 catalysts were prepared by incipient wetness impregnation using aqueous solutions of $Co(NO_3)_2\cdot 6H_2O$ as follows: The required amount of water was added to the stock solution of $Co(NO_3)_2\cdot 6H_2O$. Then, the solution was added dropwise to the γ-Al_2O_3 and TS-1 support, respectively, throughout intensive mixing. The support became slightly wet after complete addition of the solution. After the impregnation, the resulting catalyst samples were dried at 100 °C for 15 h in an oven and later calcined at 500 °C for 5 h under static air environment.

2.1 Catalyst characterization

Thermo-gravimetric Analyzer Mettler Toledo TGA/DSC-HT/1600 was used to analyze thermal stability and phase transformation of Al_2O_3, TS-1, Co/Al_2O_3 and Co/TS-1 catalyst. The samples were heated from ambient to 800 °C composition under nitrogen (N_2) gas environment at a rate of 10 °C min^{-1}.

Powder X-ray diffraction (XRD) patterns were recorded by a Rigaku Miniflex II diffractometer using Cu (Kα) radiation (lambda, λ = 0.154 nm). The data of 2 Theta (θ) were collected by means of a continuous scan mode from 10° to 80° with a sampling pitch of 0.02 and a scan rate of 4°/min. The voltage of X-ray tube was adjusted to 40 kV and the current was set at 30 mA.

Field Emission Scanning Electron Microscope (FESEM) and Energy Dispersive X-Ray (EDX), JEOL (JSM7800F) with spatial resolution up to 1 nm were used to study the surface morphology and elemental analysis of the catalyst.

Micromeritics ASAP 2020 Surface Area Analyzer was used to measure the nitrogen (N_2) adsorption-desorption isotherms at -196 °C for calcined catalysts. The samples were purged in a flow of N_2 for 3 h at 300 °C prior to the tests. The specific surface area was calculated using the BET equation.

Shimadzu UV-2600 Ultraviolet-Visible (UV-vis) spectrophotometer was used to determine the oxidation state of metal oxides on catalysts at ambient temperature in air over the range of 200 to 900 nm with reference to barium sulfate, $BaSO_4$.

Fourier transform infrared (FT-IR spectra) of the catalysts were recorded on PerkinElmer Spectrum 100 FTIR Spectrometer with a resolution of 4 cm^{-1} and 64 scans in the wavenumber region of 4000–400 cm^{-1}.

Acid-basic properties of catalysts were determined by Hammett Test, using methyl orange (H_- = 3.46),

bromocresol green (H_ = 4.9), methyl red (H_ = 5.0), phenolphthalein (H_ = 9.3), 2,4-dinitroaniline (H_=15.0), and 4-nitroaniline (H_ = 18.4) as indicators. The acid and basic strength were quantified by n-butylamine and benzoic acid titration methods respectively.

2.2 D-Glucose catalytic oxidation procedure

All D-glucose oxidations were performed in a three-neck thermostatted round bottom flask that was heated in a temperature-controlled water bath digital stirring hot plate (IKA), IKA@DTS-5 temperature controller equipped with a magnetic bar (as stirrer), under atmospheric pressure. Aqueous 1.0 M NaOH solution was titrated into the reactor to keep up constant pH throughout the reaction. Constant portions of 30 wt.% H_2O_2 solution were added manually during the course of reaction in the first hour of reaction. The required amount of H_2O_2 is based on corresponding to respective initial D-glucose concentration. The catalyst activity was studied with an initial D-glucose concentration range from 10 wt.% to 30 wt.% with constant 13.3% of H_2O_2. Approximately 16 mg catalyst was used in all experiments.

The experimental procedure was typically as follows: the reactor flask was charged with 7.5 g of an aqueous D-glucose solution in the corresponding concentration and thermostatted to the reaction temperature at 40 °C (or otherwise stated). About 13.3% total amount of H_2O_2 was added at initial time and the pH was adjusted to 9 prior to reaction initiated by the addition of the catalyst powder suspended in 0.5 g of water. As aforementioned, constant portions of H_2O_2 were added stepwise in the first hour during reaction till it reached the stoichiometric total amount, a stirring rate of 1000 rpm was employed throughout the reaction. The catalytic reaction was stopped after 5.5 h and cooled below 10 °C to stop the reaction. Samples were centrifuged at 4000 rpm for 15 min to separate the catalyst. The catalysts after reaction were separated, while the supernatant was filtered off through 0.22-μm nylon (N6).

Product analysis was carried out using HPLC on Zorbax C18 SB (250 × 4.6 mm) column, using 5 mM solution of phosphoric acid, H_3PO_4 (with pH 2.85) containing 1% acetonitrile as eluent with 1.0 mL/min flowing rate, to measure the concentration of gluconic acid, accompanied with identification by Fourier Transform Infra-Red with Attenuated Total Reflection analysis technique (FTIR-ATR). Alternatively, the glucose quantitative analysis was performed on Supercosil LC-NH_2 (250 mm × 4.6 mm) column with acetonitrile-water solution (75:25) as the eluent with 0.6 mL/min flowing rate.

Blank reaction was conducted without addition of catalyst with similar parameter. The studies on the influence of varied reaction parameters were carried out in a couple of experiments. For each tested parameter, which might be D-glucose concentrations, reaction temperature, pH, molar ratio of D-glucose to H_2O_2, and reaction time, other non-varied parameters were kept constant.

In recycling tests, the catalyst was separated by centrifugation, and washed with deionized water after each run, then reused during the subsequent run with a freshly prepared glucose solution.

In the case of H_2O_2 analysis, the amount of H_2O_2 remained after reaction of D-glucose oxidation with H_2O_2 was analytically determined by the titration technique of product solutions after reaction against potassium permanganate solution, $KMnO_4$ of known normality (N) as an indicator.

By adopting the specific calculation as listed in **Eq. (1-4)**, the conversion, selectivity and yield percent, and catalyst activity, (mmol min^{-1} g_{Co3O4}^{-1}) can be calculated accordingly with respect to all the necessary information obtained from the standard HPLC calibration curve and catalytic reaction parameters.

$$\text{Conversion \%} = \frac{\text{Total no. of mol (D-glucose + products)} - \text{No. of mol of D-glucose}}{\text{Total no. mol of (D-glucose + products)}} \times 100 \quad \textbf{(1)}$$

$$\text{Selectivity \%} = \frac{\text{No. of mol of product (Organic acid)}}{\text{Total no. of mol (D-glucose + products)} - \text{No. of mol of D-glucose}} \times 100 \quad \textbf{(2)}$$

$$\text{Yield \%} = \frac{\text{Conversion \%} \times \text{Selectivity \%}}{100} \quad \textbf{(3)}$$

$$\text{Catalyst Activity, (mmol min}^{-1}\ g_{Co3O4}^{-1}) = \frac{\text{Conversion \%} \times \text{Moles of D-glucose (mmol)}}{\text{Mass of } Co_3O_4 \text{ (g)} \times \text{Time (min)} \times 100} \quad \textbf{(4)}$$

3. Result and Discussion

3.1. Characterization of catalysts

The thermogravimetric analysis is ideally used to study the thermal stability and degradation characteristics of the catalyst samples at various temperatures and to understand the influence of calcination temperature on the characteristics of each catalyst. As the commercially ready-to-use γ-Al_2O_3 and TS-1 are usually synthesized under high temperature treatment, it is expected to be thermally stable over a high range of temperature and with low tendency of decomposition or degradation. With the introduction of Co metal, the illustration of a few small inflections at 50-200 °C in the weight loss curves of uncalcined Co/Al_2O_3 catalyst (**Fig. 1i**) expressed the endothermic loss of water molecules in the cobalt hydrate shell (**eq. 5-7**).

$$(NO_3)_2 \cdot 6H_2O \rightarrow Co(NO_3)_2 \cdot 4H_2O + 2H_2O \quad \textbf{(5)}$$

$$Co(NO_3)_2 \cdot 4H_2O \rightarrow Co(NO_3)_2 \cdot 2H_2O + 2H_2O \quad \textbf{(6)}$$

$$Co(NO_3)_2 \cdot 2H_2O \rightarrow Co(NO_3)_2 + 2H_2O \quad \textbf{(7a)}$$

$$2Co(NO_3)_2 \cdot 2H_2O \rightarrow [Co(NO_3)_2]_2O + H_2 + 3H_2O \quad \textbf{(7b)}$$

$$[Co(NO_3)_2]_2O \rightarrow 2Co(NO_3)_2 + ½\ O_2 \quad \textbf{(7c)}$$

Just after the complex dehydration process completes at around 120 °C, subsequent thermal decomposition of the nitrate anions leading to the formation of Co_3O_4 accompanied by the release of nitrogen oxides [20-22]. The single sharp peak observed at around 200 °C may be similar to the major decomposition of supported cobalt nitrate, from which leading to formation of Co_3O_4 oxide predominantly. A shoulder at slightly higher temperature of 340 °C can be identified more clearly from the derivative thermogravimetric (DTG) curve, possibly resulting from the slow desorption of gaseous product from the surface of support. The Co_3O_4 formation was confirmed by XRD analysis.

In addition, another solid residue, namely cobalt aluminate, $CoAl_2O_4$ spinel is expected to be formed as final product from decomposition of cobalt nitrate supported on Al_2O_3 leads to $CoAl_2O_4$ spinel as the final product. The formation of either Al_2O_3 and Co_3O_4 oxides mixture or $CoAl_2O_4$ spinel is found to be dependent on the support synthesis method, but the spinel formation can be implied by the highly dispersed support even in the relatively low temperature as described in the literature [23]. A further minor weight loss at around 438 °C, as illustrated in **Fig. 1i**, may be attributed to the beginning of the formation of $CoAl_2O_4$ phase in the calcined Co/Al_2O_3 catalyst. The formation of $CoAl_2O_4$ is assumed to be more substantial at 620 °C as observed from greater mass loss compared to that at 438 °C. Another possibility is that the band nearby 620 °C may be attributed to the reduction process of cobalt surface phase (CSP). Zsoldos et. al. believed that CSP phase is a hardly reducible surface phase that formed throughout calcination, covering over alumina support [24]. In addition, they assumed that this surface phase is highly dispersed and exists in the monolayer thickness in the absence of solid-state diffusion into the support matrix. Beyond these decomposition temperatures, the catalyst remained practically stable up to 800 °C. Overall, the residue of the sample is about 98.2 % (3.47 mg) which indicates a total weight loss of only 1.8 % (0.06 mg), thus, Co/Al_2O_3 catalyst is featured with high thermal stability.

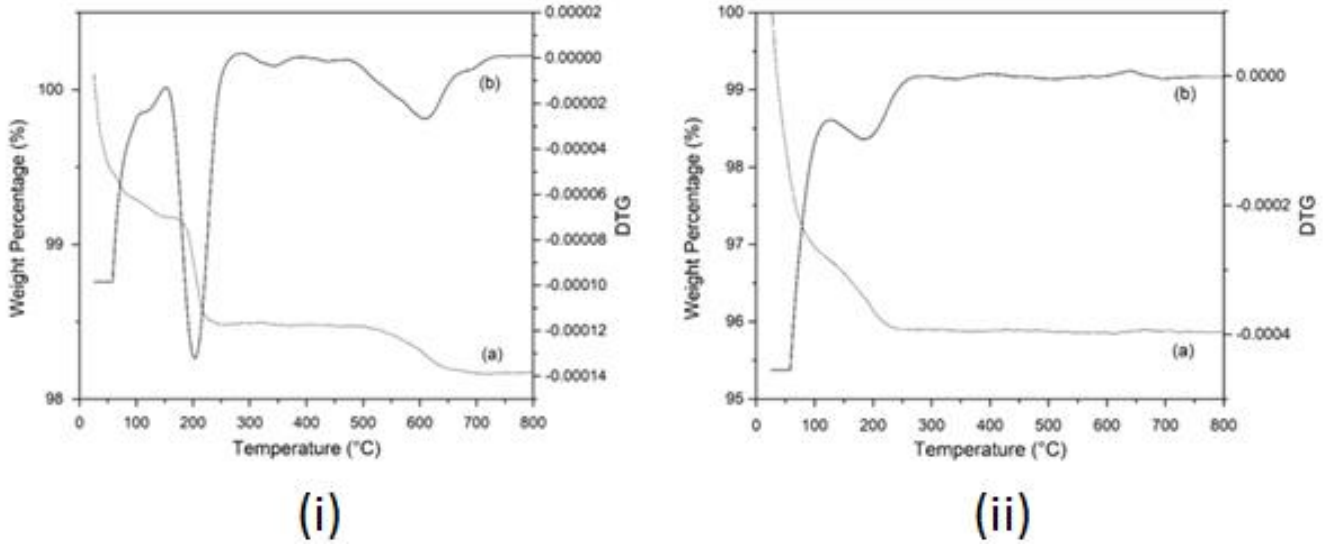

Fig. 1. TGA profile of (i) 5 wt.% Co/Al_2O_3 (ii) 5 wt.% Co/TS-1. (a) and (b) refer to Weight percentage (%) loss and derivative thermal gravimetric (DTG) respectively.

As can be seen from the thermogravimetric analysis (TGA) curve of cobalt catalyst with TS-1 support (**Fig. 1ii**), the decomposition of supported cobalt nitrate is inferred to be almost similar to alumina-supported cobalt catalyst, with major mass loss at 185 ℃ attributed specifically to the complete thermal decomposition of $Co(NO_3)_2$ predominantly to Co_3O_4 as end products. Nevertheless, on the TGA curve, the sample mass decreased slightly to 340 °C similar to that in TGA profile of Co/Al_2O_3 catalyst, which likely is owing to slow desorption of gaseous product from the surface of support. In comparison, the significant difference between the Co/TS-1 and Co/Al_2O_3 catalyst is the possibility of $CoAl_2O_4$ spinel formation in the alumina supported catalyst at high temperature treatment above 400 °C. In addition, the overall weight loss of this Co/TS-1 sample is found to be 4.0 % (0.06 mg), showing similar amount of overall mass reduction. In brief, the complete decomposition of supported cobalt nitrate mainly leads to the formation of Co_3O_4 accompanying with release of nitrogen dioxide, water and oxygen as the following overall reaction.

The XRD pattern in **Fig. 2** illustrates that Co/Al_2O_3 catalyst indicates all the characteristic peaks of γ-Al_2O_3. The diffraction peaks presence at 2θ = 31.3°, 36.9° and 65.5° may be attributed to either Co_3O_4 or $CoAl_2O_4$ species as both Co_3O_4 and $CoAl_2O_4$ have a cubic spinel structure with almost the same XRD patterns [25-27]. However, the appearance of the peak at 2θ = 36.9°, significantly evidences the presence of Co_3O_4 crystallites. All the initial Co (II) oxide is completely consumed as indicated by the absence of a distinct CoO_x phase from the XRD analysis. The low intensity of cobalt oxide crystallites indicates that they present in a highly dispersed form on alumina support, which is in good agreement with EDX mapping results.

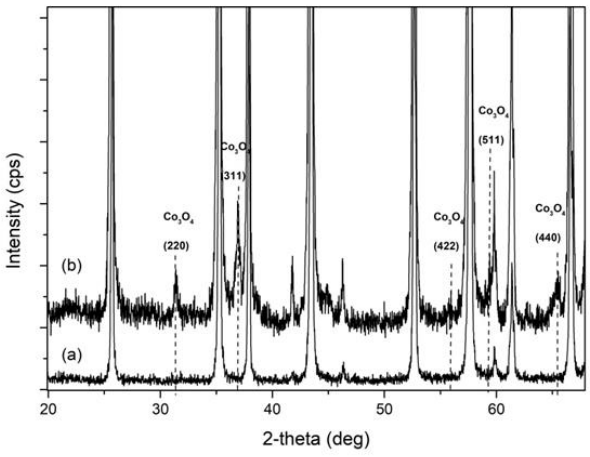

Fig. 2. XRD patterns of (a) γ-Al_2O_3 and (b) calcined 5 wt.% Co/Al_2O_3.

XRD analysis for both calcined TS-1 and Co/TS-1 catalysts showed diffraction peaks at 2θ = 23.2°, 23.8°, 24.5°, 29.2° and 45° as depicted in **Fig. 3**. This revealed that the introduction of cobalt metal did not alter the TS-1 intrinsic MFI zeolitic structure since only a similar set of diffraction peaks characteristic of the MFI configuration were shown ascribed to TS-1 [28]. The calcined TS-1 has orthorhombic symmetry with characteristic single reflections around 2θ = 24.5° and 29.2°, which indicate Ti located in the zeolite framework [29]. No diffraction peak around 2θ = 25.4° was observed, suggesting the absence of extra-framework of crystalline TiO_2 (anatase) in the catalysts and all Ti species were located inside molecular sieve of TS-1 [30]. The absence of CoO_x crystalline diffraction peaks is due to similar reason as stated for Alumina supported catalyst.

Fig. 4 depicts FESEM images of synthesized catalyst with 5 wt% Co supported on Al_2O_3 and TS-1, respectively. The analysis revealed the results of surficial morphology and assessment of particle size of the samples. Size analyzer of FESEM images prove that the particles contained are in nanometric and micrometric scales. Al_2O_3 as support material are a well ordered flower-like plate structure (**Fig. 4a**), whereas the addition of Co on Al_2O_3 affect the morphology features of the catalyst, this can be observed by the comparison of the surficial properties (**Fig. 4b**). In case of TS-1 as a support material, incorporation of Co illustrates an almost similar morphological structure with a uniform particle size (**Fig. 4c** and **4d**). Elemental analysis using Energy-dispersive X-ray (EDX) shows almost identical to theoretical value of Co (5.27 wt.%) for Co/TS-1 catalysts, whereas 8.13 wt.% was obtained for Co/Al_2O_3 sample. Additional dot map micrographs prove that Co is uniformly dispersed and no visible particles agglomeration are observed on the surface of supported materials.

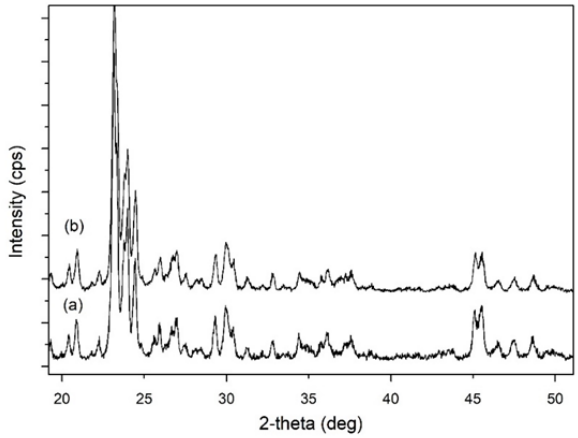

Fig. 3. XRD patterns of (a) TS-1 and (b) calcined 5 wt.% Co/TS-1.

The BET surface area, total pore volume, mean pore diameter of the γ-Al_2O_3, Co/Al_2O_3, TS-1 and Co/TS-1 catalysts were determined by N_2 adsorption and desorption isotherms analysis, with results shown in **Table 1**. In both supports, the addition of Co does not alter the BET surface area. The surface area of Co modified alumina catalyst remained around 1.6 m^2/g as exhibited by γ-Al_2O_3 whereas the total pore volume of Co/Al_2O_3 (0.007 cm^3/g) is almost doubled to that of γ-Al_2O_3 (0.004 cm^3/g). On the other hand, both the TS-1 and Co modified TS-1 catalysts possess a surface area of about 415.0 m^2/g and the total pore volume of 0.310 cm^3/g. N_2 adsorption-desorption isotherm plot illustrated that both cobalt supported catalysts exhibit mesoporous structure with well-dispersion of metal oxides crystallites, and their main difference is that Co/TS-1 may comprise some micropores (**Fig. S1**).

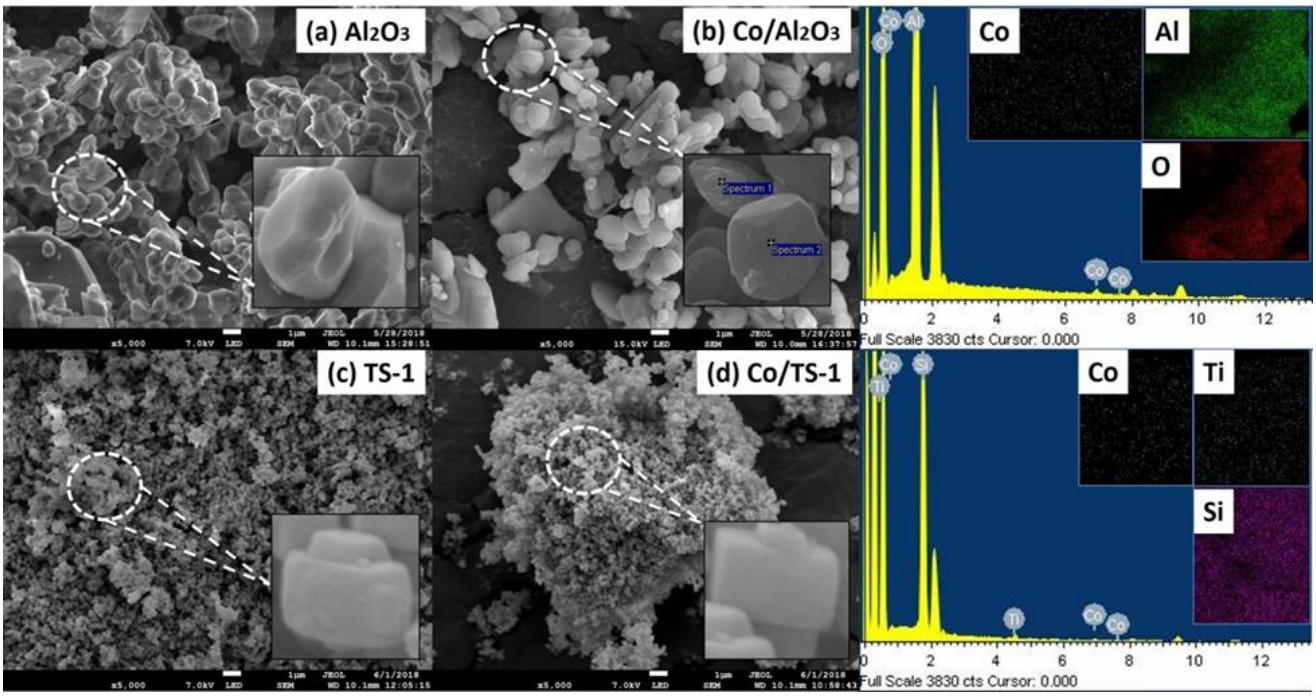

Fig. 4. FESEM images of synthesized catalysts that have undergone a calcination process, at 500 °C: (a) γ-Al_2O_3, (b) 5 wt.% Co/Al_2O_3 with EDX analysis, (c) TS-1, (d) 5 wt.% Co/TS-1 with EDX analysis.

Table 1. N_2-physisorption analysis of catalysts.

Catalyst	Co metal (wt.%)	BET surface area (m^2/g)	Total pore volume (cm^3/g)	Pore size (nm)
Al_2O_3	-	1.6	0.004	9.3
Co/Al_2O_3	5	1.7	0.007	15.7
TS-1	-	415.4	0.306	2.9
Co/TS-1	5	419.3	0.320	3.0

The spectrum of the calcined Co/Al_2O_3 catalyst (**Fig. 5**) shows two broad and intensive absorption bands at around 431 nm and at 718 nm which specifies the presence of cobalt phases, wherein substantial cobalt atoms exist in symmetries of octahedral and tetrahedral [31]. The Co^{2+} ions are both tetrahedrally and octahedrally coordinated in Co_3O_4 particles dispersion. According to TGA analysis, the $CoAl_2O_4$ species is expected to present when the catalyst is exposed to calcination at 500 °C. However, no adsorption peaks attributed to $CoAl_2O_4$ species were found in the as-prepared catalyst as evidenced by the absence of a characteristic distorted triplet adsorption band near 620 nm corresponding to tetrahedral Co^{2+} and the other absorption band at 350 nm. This result confirmed the absence of $CoAl_2O_4$ species, clarifying XRD analysis. In brief, the dominant Co_3O_4 species is expected to play a vital role in the oxidation reaction [32].

As shown in **Fig. 6**, the appearance of intense absorption bands at 220 nm are noticeable in the spectra for TS-1 and 5 wt.% Co/TS-1 (uncalcined and calcined) samples, which signifies that the titanium (Ti) was incorporated in the TS-1 framework [33]. CoO_x oxide is expected to present in the calcined Co/TS-1 as deduced from the two significant broad peaks located in the respective ranges of 280–450 nm and 560–700 nm is probably corresponding to ultraviolet absorbances of CoO_x oxide. This can prove that the TS-1 surface of catalysts is highly dispersed with very small CoO_x crystallites, confirming the presence of Co_3O_4 crystallites, though they are unnoticeable in XRD.

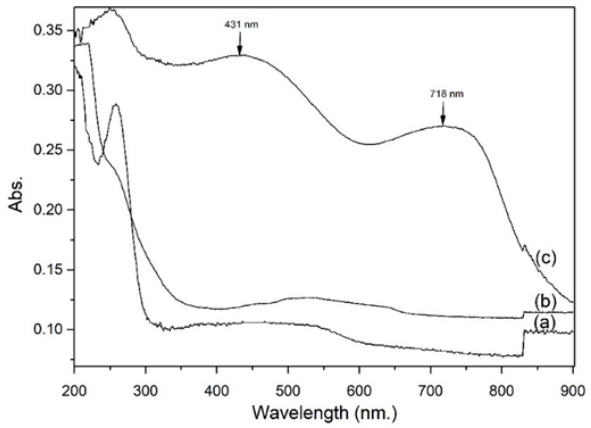

Fig. 5. UV-Vis-NIR spectra of (a) Calcined γ-Al_2O_3, (b) Uncalcined 5 wt.% Co/Al_2O_3, (c) Calcined 5 wt.% Co/Al_2O_3.

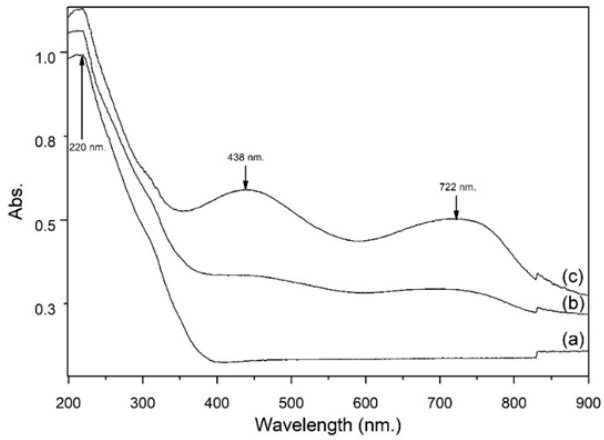

Fig. 6. UV-Vis-NIR spectra of (a) Calcined TS-1, (b) Uncalcined 5 wt.% Co/TS-1, (c) Calcined 5 wt.% Co/TS-1.

FTIR spectra of γ-Al_2O_3 and Co/Al_2O_3 catalysts illustrated the presence of hydroxyl group from an adsorption band at around 3433 cm^{-1} which is attributed to the O–H stretching mode vibrations (**Fig. 7**). Within the region of 800-500 cm^{-1}, strong doublet peaks near 657 and 608 cm^{-1} are characteristic assignment of metal oxygen vibrations in the cubic Co_3O_4 oxide (spinel) as reported in previous study [34]. The presence of water in samples is recognized from the peak of water bending mode at around 1641 cm^{-1}. Since there is no shift in the O-H and metal-oxygen stretching bands toward higher wavenumber regions (particularly at 3445 and 676 cm^{-1} respectively) attributed to the $CoAl_2O_4$ phase as indicated in the literature data [35], verifying that the absence of $CoAl_2O_4$ spinel is in good agreement with the UV-Vis-NIR results.

The FTIR spectra of TS-1 and Co/TS-1 catalysts showed the strongest absorption bands at around 1100 cm^{-1} with a shoulder at 1230 cm^{-1} is particularly assigned to asymmetric stretching of Si–O–Si; the bands near 803 cm^{-1} is attributed to bending or stretching of SiO–Si bridge; and the bands at 552 cm^{-1} belongs to Si–O–Si rocking (**Fig. 8**). These characteristic peaks also revealed the MFI structure of zeolite and the Co modified catalyst remained intact as TS-1 structure, which is consistent with the XRD results. A characteristic peak near 970 cm^{-1} is generally ascribed to [SiO_4] tetrahedral bond stretching vibration in the O_3Si–O–Ti structure, indicating the incorporation of Ti into the framework of zeolite.

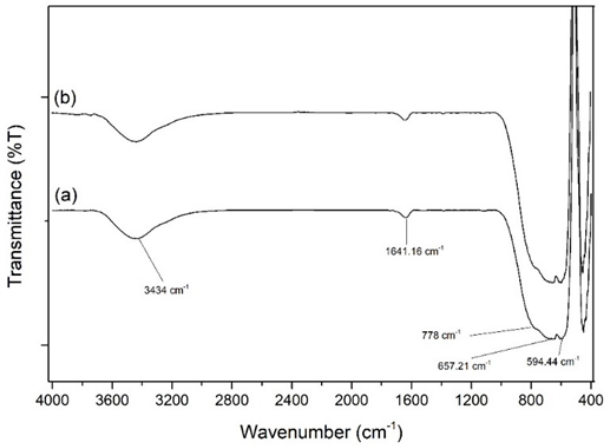

Fig. 7. FTIR spectra of (a) γ-Al_2O_3 and (b) 5 wt.% Co/Al_2O_3 catalyst

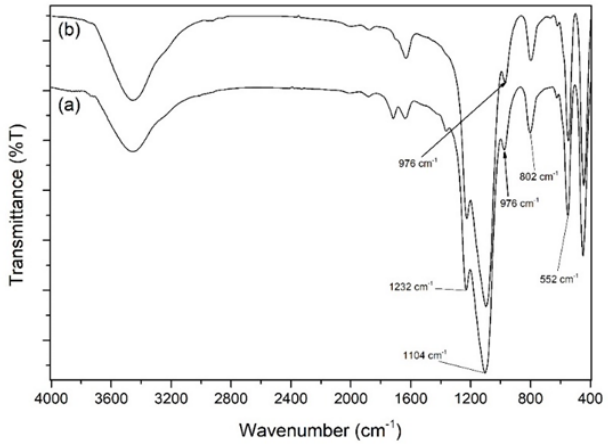

Fig. 8. FTIR spectra of (a) TS-1 and (b) 5 wt.% Co/TS-1 catalysts.

The overall acido-basic properties of the catalysts are tabulated in **Table S1**. By observing the color changes of Hammett indicators, both Al_2O_3 and Co/Al_2O_3 are indicated as neutral exhibiting both acidic and basic sites, whereas TS-1 and Co/TS-1 are slightly acidic in nature. Thereafter, the acidity values of the catalysts were measured by n-butylamine titration method using different Hammett indicators with pKa ≤ +6.8, while the basicity values of the catalysts were measured through

benzoic acid titration technique using other indicators with pKa ≥ + 7.2. In comparison, TS-1 is assumed to occupy more acidic sites on catalyst surface than the others, whereas Co/TS-1 became slightly basic with the introduction of Co. Nevertheless, Hammett indicator method was limited for the accurate measurement of the acidity and basicity of the catalyst, regarding the total of Lewis acid and base, and Brönsted acid and base.

3.2. Catalysts Activity

The selective oxidation of the D-glucose into D-gluconic acid with improved yield and selectivity has been achieved in the presence of a cobalt catalyst, comprising particles of cobalt species dispersed on a support (i.e., Co/Al_2O_3 and Co/TS-1), as compared to the uncatalyzed reaction as well as the catalyzed reactions solely by alumina and titanium silicate-1 catalysts (**Table 2**). In this study, through HPLC analyses and standard solution as reference, D-glucose was anticipated as selectively converting to D-gluconic acid predominantly, rather than to other possible oxidation products, i.e. glucaric acid, glucuronic acid and other organic acids through similar catalytic route. Besides, the HPLC analysis confirmed the absence of isomerization of glucose to fructose.

In catalyzed reaction, the activation of H_2O_2 is likely to take place mediated by Co crystallites, where homolytic decomposition of H_2O_2 occurs with one-electron redox couples of Co(II)/Co(III) of Co_3O_4 spinel [36, 37]. This mechanism generates hydroxyl radicals (HO·) and peroxyl radicals (HOO·) and/or high-valent oxometal species as active oxidant, thereby producing active oxygen to competently react with D-glucose adsorbed on the catalyst surface. By comparing the cobalt supported catalysts, the Co/Al_2O_3 catalyst has achieved D-gluconic acid yield of 63.3 % which is higher than Co/TS-1 catalyst which gave slightly lower yield of 53.7 % D-gluconic acid.

Table 2. Catalytic data for oxidation of D-glucose under prescribed standard reaction conditions. *

Reaction	Conversion (%)	Selectivity (%)	Yield (%)
Blank	65.1	61.3	39.9
TS-1	60.1	51.0	30.7
γ-Al_2O_3	64.6	54.1	34.9
Co/TS-1	53.8	100.0	53.7
Co/Al_2O_3	63.3	100.0	63.3

*Reaction conditions: D-glucose concentration, 30 wt.%; catalyst, 16 mg; Temperature, 40 °C; pH, 9; D-glucose: H_2O_2, 1:1.0 (Molar ratio); Standard stirring rate, 1000 rpm; Reaction time, 5.5 h

From the viewpoint of catalyst properties, the catalyst performance is expected to be dependent on nature of support. The Co/Al_2O_3 catalyst is suggested to exhibit greater ability to adsorb the active oxygen species produced as H_2O_2 activated on the catalyst surface, as well as better adsorption of D-glucose, on account of its strong lateral adsorbate interactions with adsorbed layer as depicted by nitrogen (N_2) physisorption. Indeed, the Co/Al_2O_3 catalyst showed a more distinct presence of Co_3O_4 phase under XRD and UV-Vis-NIR spectra as compared to Co/TS-1 counterpart, thus facilitates formation of active oxygen species which is crucial for D-glucose selective oxidation. Considering the other catalytic features, the acidity of the materials may have a negative influence on the alkaline-conditioning reaction to certain extent, since TS-1 is considered to have more acidity than Al_2O_3. It is expected Co/Al_2O_3 exhibit conjugated basic site to activate the primary hydroxyl group on glucose to form gluconic acid. The 5 wt.% Co/Al_2O_3 was then the catalyst of choice by virtue of its catalytic capability.

3.2.1 Influence of H_2O_2 Addition Procedure on Catalytic activity

One-pot addition of H_2O_2 was practically applied by most of the researchers in earlier investigations on oxidation of D-glucose with H_2O_2. However, as per Ishida et. al. [6] reported, a markedly lower D-glucose conversion of <50 % was mostly obtained by way of one-pot addition of excess H_2O_2, whereas Saliger et. al. [7], in contrast, obtained a D-glucose conversion of > 99 % by employing a subsequent step-wise addition of a total stoichiometric amount of H_2O_2 relating to D-glucose in the course of the reaction. In order to verify the effect of H_2O_2 addition procedure on H_2O_2 performance, the selective catalytic oxidation of D-glucose in this section was carried out by both the one-pot and step-wise H_2O_2 addition with the use of Co/Al_2O_3 catalyst. The D-glucose oxidation reaction with step-wise addition of H_2O_2 was carried out as described in section 3.5, whereas, for the reaction with one-pot H_2O_2 addition, only one portion of total 1.50 mL H_2O_2 was added into the reactor without prior addition of the initial H_2O_2.

In line with the Saliger et. al. [7] study, higher D-glucose conversion and D-gluconic acid yield of 54.4% was obtained with step-wise addition of H_2O_2 as compared to that with one-pot addition of H_2O_2 which only gave a yield of 40.8%. It is suggested that the low conversion may probably be due to the leakage of O_2 formed, via H_2O_2 decomposition, out of the reactor. This phenomenon can also be known as gas evolution successive to H_2O_2 decomposition. Gas evolution

generally occurs when the concentration of H_2O_2 is too high in comparison to the concentration of D-glucose. In this instance, H_2O_2 is decomposed substantially faster to H_2O and O_2 than its reaction with D-glucose. The prevalence of oxygen leakage is more likely to occur with one-pot H_2O_2 addition, whereby the yield % of D-gluconic acid corresponding to its D-glucose conversion increased remarkably only at initial time. In contrast, in the reaction with step-wise addition of H_2O_2, the D-glucose conversion increased gradually over time towards a higher yield of D-gluconic acid. Nonetheless, a complete conversion of D-glucose in oxidation reaction applied with the step-wise addition of H_2O_2 is yet to be achieved. Hence, oxygen leakage may also occur to a certain extent, and further investigations on influence of other experimental reaction parameters are needed.

3.2.2. Influence of D-glucose concentration

The influence of varied initial D-glucose concentration on D-glucose oxidation with H_2O_2 was examined in the range of 10–30 wt.%. A constant catalyst load 16 mg of 5wt% Co/Al_2O_3 was used in all experiments in this section. As shown in **Table 3**, an increase of total yield of D-gluconic acid is obtained with an increase of catalyst activity with a rise in D-glucose concentration up to 30 wt.%. Thus, indicating that the tested catalytic system able to efficiently catalyzed the reaction with minimum effect on the oxygen solubility issues faces by most of the works with molecular oxygen as oxidant. In their case, the optimum workable of D-glucose concentration is around 20 wt.%. In general, the variation of the D-glucose concentration did not affect the total selectivity to D-gluconic acid in the present study and no by-products were detected by HPLC.

Table 3. Catalyst activity and D-gluconic acid yield in dependence on the D-glucose concentration. *

D-glucose Concentration (wt.%)	Substrate-to-catalyst ratio ($q = C_o/C_c$)	Activ. (mmol min^{-1} g_{Co3O4}^{-1})	Select. (%)	Yield (%)
10	306.8	1011	100	26.1
20	573.8	3109	100	43.0
30	920.3	5083	100	43.8

*Reaction conditions: 5wt% Co/Al_2O_3, 16 mg; Temperature, 40 °C; pH, 9; D-glucose: H_2O_2, 1:1.0 (Molar ratio); Standard stirring rate, 1000 rpm; Reaction time, 5.5 h

3.2.3 Influence of Reaction Temperature

The effect of the reaction temperature on D-glucose oxidation with H_2O_2 was studied in the range of 30–60 °C. The temperatures above 60 °C were not studied in this work because low selectivity to D-gluconic acid is generally resulted by the presence of by-products owing to the occurrence of homogenous reactions of D-glucose such as isomerization and degradation [14]. The dependency of catalyst activities on reaction temperature are shown in **Fig. 9**. Catalyst activity strongly increases with rising reaction temperature, from which relatively high yield (72.4%) of targeted product is realized at 60 °C. An Arrhenius plot was established as **Fig. 10** based on the catalyst activities presented in **Fig. 9**. The apparent activation energy calculated from logarithm form of Arrhenius equation ($k=Ae^{-Ea/RT}$) was found to be 15 kJ mol^{-1} approximately which is lower compared to the value obtained from a comparable reaction in the presence of Au based catalytic system [7]. The appreciable difference in activation energies of these catalysis systems may be caused by the difference in the adsorption abilities of catalyst for glucose [38], according to the nature of catalyst surface and electronic properties, attributable to different nanostructures [39-41].

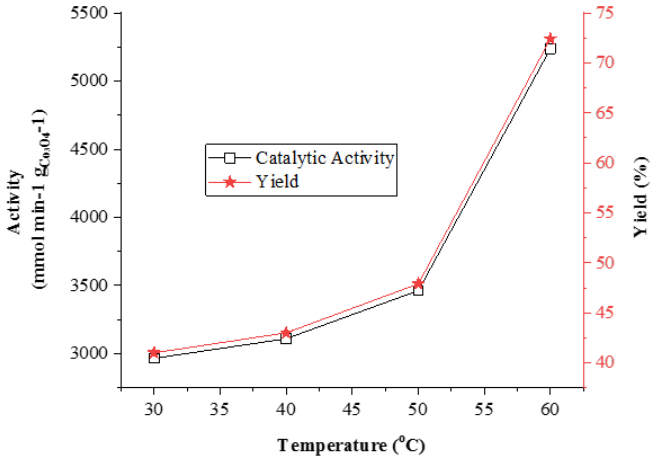

Fig. 9. Catalyst activity in dependence on the reaction temperature. Reaction conditions: D-glucose concentration, 20 wt.%; 5 wt% Co/Al_2O_3, 16 mg; pH, 9; D-glucose: H_2O_2, 1:1.0 (Molar ratio); Standard stirring rate, 1000 rpm; Reaction time, 5.5 h.

3.2.4. Influence of pH

D-glucose oxidation with H_2O_2 was further studied under slightly acidic and neutral conditions at pH 5 and 7, respectively. The results were compared to the standard reaction at pH 9 and are reported in **Fig. 11**.

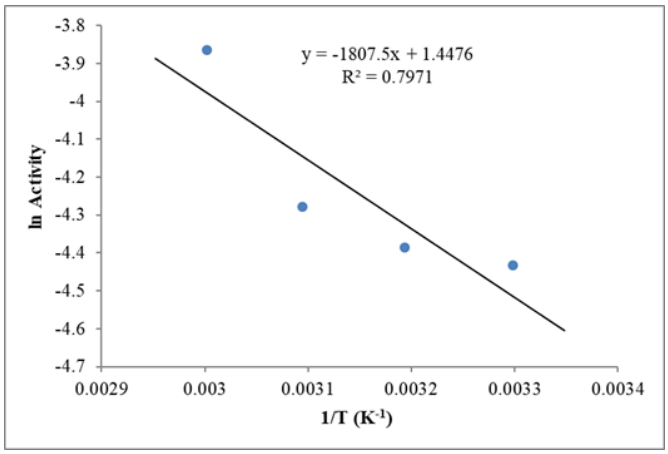

Fig. 10. Arrhenius plot for the determination of apparent activation energy.

In contrast, the catalyst activity under slightly alkaline conditions (pH 9) was significantly higher than that in acidic conditions. Highest D-glucose conversion of 72.4% is attained at pH 9, while lower conversion of 65.2 % was reached in pH 5 after 5.5 h. The activity of catalyst was expectedly higher at pH 7 to some extent as compared to pH 5, which gives somewhat higher conversion of 67.7%. This is commonly concerning deprotonation of substrate at pH> 7, thus faster desorption of gluconic acid. Lower conversion and catalyst activity at pH< 7 tends to signify a catalyst deactivation attributed to undissociated D-gluconic acids which remain adsorbed on the catalytic active sites of the noble metal and poses catalyst self-poisoning [42]. Other unknown organic acids are more likely to form; as alkaline degradation may be dominant over oxidation to gluconic acid.

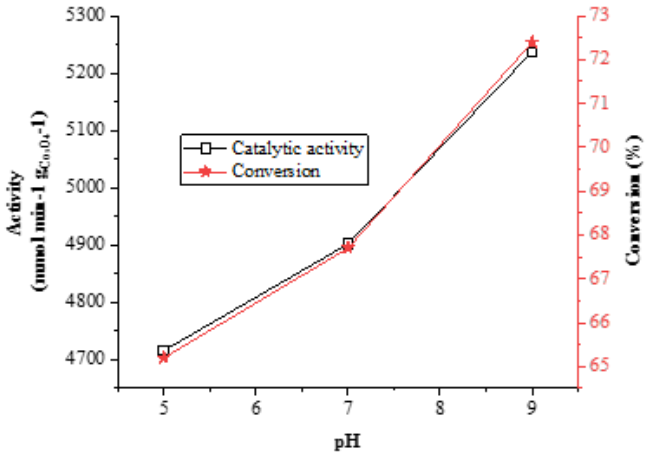

Fig. 11. Catalyst performance in dependence on the reaction pH value. Reaction conditions: D-glucose concentration, 20 wt.%; 5 wt% Co/Al_2O_3, 16 mg; Temperature, 60 °C; D-glucose: H_2O_2, 1:1.0 (Molar ratio); Standard stirring rate, 1000 rpm; Reaction time, 5.5 h.

3.2.5. Influence of D-glucose to Hydrogen Peroxide Molar Ratio

The investigation on whether a stoichiometric amount of H_2O_2 (1.0 equiv.) in relation to D-glucose could sufficiently bring about a complete D-glucose conversion was first performed. Then, the effect of varied D-glucose to H_2O_2 molar ratio towards D-gluconic acid formation was also studied and the results are reported in **Fig. 12**. Higher conversion and yield of D-gluconic acid are achievable with the increased molar ratio of H_2O_2 to D-glucose. This is often attributed to the shift of equilibrium towards the side reaction ($H_2O_2 + 2\ H^+ + 2\ e^- \rightarrow 2\ H_2O$) through the introduction of excess amounts of H_2O_2 oxidizing agents. The activity value and D-glucose conversion at stoichiometric ratio were doubled to those at 1:0.5 D-glucose to H_2O_2 molar ratio, but there is no remarkable increase in activity and D-glucose conversion as well as the yield of D-gluconic acid with molar ratio of D-glucose to H_2O_2 up to 1:3.0. Furthermore, the selectivity to D-gluconic is not significantly influenced by the variation of the D-glucose to H_2O_2 molar ratio. As the excess of H_2O_2 even in a small amount is unfavorable with reference to the costs, the stoichiometric amount of H_2O_2 in relation to D-glucose is still in preference for the optimum, cost-effective process. The decomposition of H_2O_2 was also studied by determining the amount of H_2O_2 that remained based on procedure mentioned in [43]. Almost all H_2O_2 decomposed under the slightly alkaline condition (pH 9) in the first hour; immediately after the total amount of H_2O_2 has been added. According to Salinger et al [7], under high concentration of hydrogen peroxide, the decomposition of H_2O_2 oxidant to form H_2O and O_2 is considerably faster than its reaction with d-glucose subsequently influence catalytic activity.

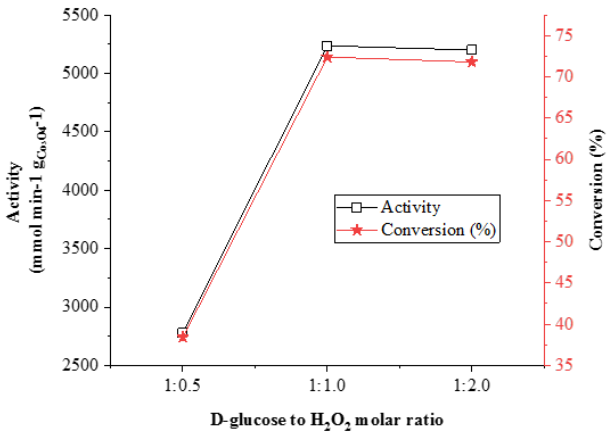

Fig. 12. Catalyst activity and D-glucose conversion and yield of product at different D-glucose to H_2O_2 molar ratio. Reaction conditions: D-glucose concentration, 20 wt.%; 5 wt% Co/Al_2O_3, 16 mg; Temperature, 60 °C; pH, 9; Standard stirring rate, 1000 rpm; Reaction time, 5.5 h.

3.2.6. Influence of Reaction Duration

The time-course of D-gluconic acid yields was investigated, complemented with the study on D-glucose conversion and selectivity to D-gluconic acid during D-glucose oxidation with H_2O_2 over 5 wt.% Co/Al_2O_3 via Time-online analysis (TOL). The TOL statistics give a picture of linear increment in D-gluconic acid yield up to 81.3% at 3 h, attained with high catalyst activity of 10792 mmol min^{-1} g_{Co3O4}^{-1}, reaching a plateau after 3 h (**Fig. 13**). Lower D-glucose conversion observed at prolonged reaction time might be due to the limiting amount of adsorbed active oxygen species from H_2O_2 decomposition on the catalyst surface and/or slower rate of D-gluconic acid desorption from the catalyst surface. Hence the catalyst presumed saturated with end products at the time, causing lower catalytic activity of catalyst, and desorption of unreacted D-glucose from catalyst into solution. Accordingly, TOL analysis reflects that 3 h reaction time is considered as the most optimum time for favorable production of D-gluconic acid with the presence of cobalt supported Al_2O_3 catalyst.

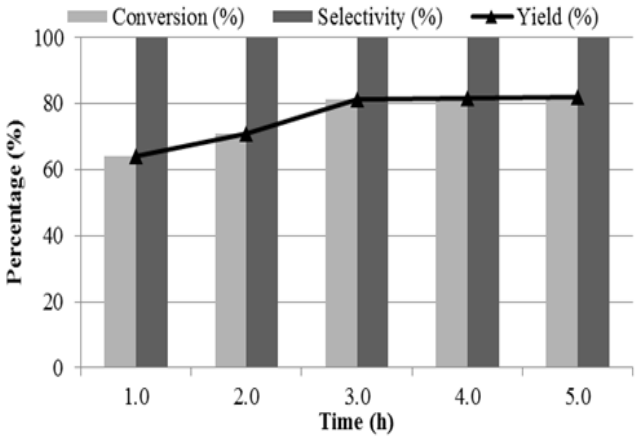

Fig. 13. The time-course of D-glucose conversion (%), D-gluconic acid selectivity (%) and D-gluconic acid yield (%). Reaction conditions: D-glucose concentration, 20 wt.%; 5 wt% Co/Al_2O_3, 16 mg; Temperature, 60 °C; pH, 9; D-glucose: H_2O_2, 1:1.0 (Molar ratio); Standard stirring rate, 1000 rpm.

3.3. Reusability of the 5 wt.% Co/Al_2O_3 catalyst in the D-glucose oxidation

In addition to high efficacy, long-term reusability is likewise one of the essential properties for establishing an industrial-used catalyst. Herein, the reusability of Co/Al_2O_3 was studied by performing the recyclability tests of the catalyst under the optimized standard reaction conditions towards the synthesis of D-gluconic acid. The very low percent drop in D-glucose conversion and yield of D-gluconic acid with no notable changes in selectivity were observed in three consecutive cycles, indicating that the catalyst is able to retain optimal performance at each cycle of study (**Fig. 14**). Thus, the catalyst at certain extent might resist the possible inhibitory effect by ketone related intermediates and condensation products possibly formed from glucose under alkaline environment. However, close observation on FTIR spectra of spent catalyst illustrates sharper intensity of the peaks near 3446 cm-1 and 1635 cm-1 are typically due the presence of hydroxyl groups O–H, which probably indicates the attendance of unconverted D-glucose and products molecules (**Fig. S2**). In addition, the band at 2923 cm^{-1} is assigned to the C–H and C–H_2 stretching; the peak near 1413 cm^{-1} belongs to asymmetric stretching of O–C–O; and the band around 1085 cm-1 is attributed to C–O stretching. All these peaks are typically characteristics of D-gluconic acid. On the other hand, the characteristics band at 2850 cm^{-1} that is recognized as C–H stretching of both α- and β- anomers reveals the presence of D-glucose. Thus, this might inhibit interaction between active sites and reactants; and subsequently affect the catalytic activity of spent catalyst. However, qualitative acid-basic properties of spent 5 wt.% Co/Al_2O_3 catalyst were analyzed via Hammett Test and values are presented in **Table 4**. Results demonstrate catalytic property analogous to fresh 5 wt.% Co/Al_2O_3 catalyst.

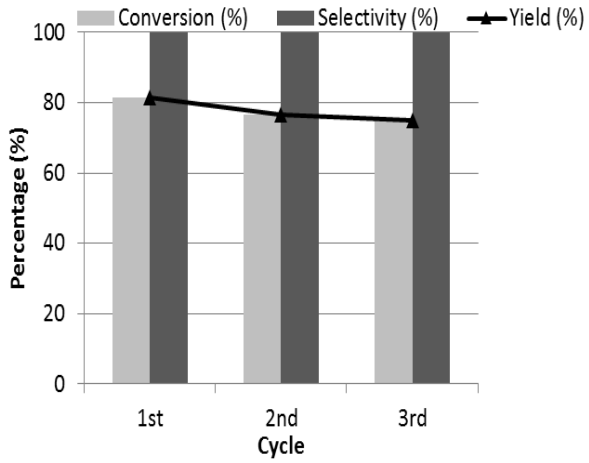

Fig. 14. Reusability study of Co/Al_2O_3 on glucose conversion, gluconic acid selectivity and yield. Reaction conditions: D-glucose concentration, 20 wt.%; 5 wt% Co/Al_2O_3, 16 mg; Temperature, 60 °C; pH, 9; D-glucose: H_2O_2, 1:1.0 (Molar ratio); Standard stirring rate, 1000 rpm; Reaction time, 3 h.

4. Conclusions

The present work aims to selectively synthesis D-gluconic acid via D-glucose oxidation using H_2O_2 oxidant over a supported non-noble metal heterogeneous catalyst, in accordance with the principl-

Table 4. Measurement of acid-basic properties of 5 wt. % Co/Al_2O_3 using Hammett test.

Catalyst	Methyl orange (H_=3.7)	Bromo-cresol Green (H_=4.9)	Methyl red (H_=5.0)	Phenolphthalein (H_=8.2)	2,4-dinitro-aniline (H_=15.0)	4-nitro-aniline (H_=18.4)
Fresh, 5 wt.% Co/Al_2O_3	No changes	No changes	No changes	No changes	No changes	No changes
Spent 5 wt.% Co/Al_2O_3	No changes	No changes	No changes	No changes	No changes	No changes

-es of green and sustainable chemistry for catalytic oxidation processes. Co/Al_2O_3 catalyst is particularly active for the liquid-phase oxidation of D-glucose, with enhanced selectivity to D-gluconic acid of about 100% under most applied reaction conditions in the study. It suggested synergistic effect between Co crystallites and Al_2O_3 support, where the Co_3O_4 phase mediated H_2O_2 decomposition, releasing active oxygen molecule, while Al_2O_3 provides active sites for the activation of glucose molecules. The Co/Al_2O_3 catalyst has good catalyst activity of 10792 mmol min^{-1} $g_{Co3O4}{}^{-1}$. The apparent activation energy in the range of 30–60 °C is comparatively lower than the average value reported for gold-based catalyst for the oxidation of D-glucose using H_2O_2 oxidant. This suggested a difference in mechanism and catalyst structure properties. Further, Co/Al_2O_3 catalyst is reusable with optimal catalytic performance at each cycle of study.

Acknowledgements

The authors are grateful to University Malaysia Pahang, Malaysia for Internal Grants Research Scheme (RDU1703277) and Doctoral Research Scheme (DRS) Scholarship.

References

[1] X. Zhang, K. Wilson, A. F. Lee, Chem Rev. 116 (2016) 12328-12368.
[2] S. Ramachandran, P. Fontanille, A. Pandey, C. Larroche, Food Technol Biotech. 44 (2006) 185-195.
[3] A. Cañete-Rodríguez, I. Santos-Dueñas, J. Jiménez-Hornero, A. Ehrenreich, W. Liebl, I. García-García, Process Biochem. 51 (2016) 1891-1903.
[4] P. Pal, R. Kumar, S. Banerjee, Front Chem Sci Eng. 13 (2019) 152-163.
[5] S. Anastassiadis, I. G. Morgunov, Recent Pat Biotechnol. 1 (2007) 167-180.
[6] T. Ishida, K. Kuroda, N. Kinoshita, W. Minagawa, M. Haruta, J. Colloid Interface Sci. 323 (2008) 105-111.
[7] R. Saliger, N. Decker, U. Prüße, Appl. Catal. B. 102 (2011) 584-589.
[8] B. N. Zope, D. D. Hibbitts, M. Neurock, R. J. Davis, Science. 330 (2010) 74-78.
[9] S. E. Davis, B. N. Zope, R. J. Davis, Green Chem. 14 (2012) 143-147.
[10] M. Moo-Young, Comprehensive biotechnology, third ed., Elsevier, 2019.
[11] P. Pal, R. Kumar, S. Banerjee, Chem Eng Process. 104 (2016) 160-171.
[12] I. Dencic, J. Meuldijk, M. de Croon, V. Hessel, J. Flow Chem. 1 (2012) 13-23.
[13] T. Haynes, O. Ersen, V. Dubois, D. Desmecht, K. Nakagawa, S. Hermans, Appl. Catal. B. 241 (2019) 196-204.
[14] A. Mirescu, H. Berndt, A. Martin, U. Prüße, Appl Catal A-Gen. 317 (2007) 204-209.
[15] A. M. Velarde, P. Bartl, T. Nießen, W. Hoelderich, J. Mol Catal A Chem. 157 (2000) 225-236.
[16] M. Khawaji, Y. Zhang, M. Loh, I. Graça, E. Ware, D. Chadwick, Appl. Catal. B. 256 (2019) 117799-117811.
[17] S. M. Lama, J. Schmidt, A. Malik, R. Walczak, D. V. Silva, A. Völkel, M. Oschatz, ChemCatChem. 10 (2018) 2458-2465.
[18] Y. Zhuge, G. Fan, Y. Lin, L. Yang, F. Li, Dalton Trans. 48 (2019) 9161-9172.
[19] X. Zhang, H. Shi, Q. Chi, X. Liu, L. Chen, Polym Bull. 77 (2020) 1003-1014.
[20] C. Ehrhardt, M. Gjikaj, W. Brockner, Thermochim. Acta. 432 (2005) 36-40.
[21] D. Ghita, D. S. Ezeanu, P. Rosca, D. Cursaru, Rev. Chim. (Bucharest). 65 (2014) 1395-1398.
[22] B. Małecka, A. Łącz, E. Drożdż, A. Małecki, J Therm Anal Calorim. 119 (2015) 1053-1061.
[23] P. Bolt, F. H. Habraken, J. Geus, J. Solid State Chem. 135 (1998) 59-69.
[24] Z. Zsoldos, F. Garin, L. Hilaire, L. Guczi, J Mol Catal A Chem. 111 (1996) 113-122.
[25] L. P. Profeti, E. A. Ticianelli, E. M. Assaf, J. Power Sources. 175 (2008) 482-489.
[26] C. Cheng, S. Foo, A. Adesina, Catal Commun. 12 (2010) 292-298.
[27] R. Padilla, M. Benito, L. Rodríguez, A. Serrano, G. Muñoz, L. Daza, Int J Hydrogen Energ. 35 (2010) 8921-8928.

[28] L. Cumaranatunge,W. N. Delgass, J. Catal. 232 (2005) 38-42.
[29] M. Taramasso, G. Perego, B. Notari, Patent (1983), 4 410 501. 1981.
[30] Y. S. Ko,W. S. Ahn, Korean J Chem Eng. 15 (1998) 182-191.
[31] L. P. Profeti, E. A. Ticianelli, E. M. Assaf, Fuel. 87 (2008) 2076-2081.
[32] S. Albonetti, R. Mazzoni, F. Cavani (Eds.), Homogeneous, Heterogeneous and Nanocatalysis, RSC, 2014, 1-39.
[33] S. Laha, R. Kumar, J. Catal. 208 (2002) 339-344.
[34] L. Ji, J. Lin, H. Zeng, J. Phys. Chem. B. 104 (2000) 1783-1790.
[35] G. Busca, V. Lorenzelli, V. Bolis, Mater. Chem. Phys. 31 (1992) 221-228.
[36] E. S. Spier, I. Hermans. ChemPhysChem. 14 (2013) 3384-3388.
[37] S. J. Arts, E. J. Mombarg, H. van Bekkum, R. A. Sheldon, Synthesis. 1997 (1997) 597-613.
[38] H. Okatsu, N. Kinoshita, T. Akita, T. Ishida, M. Haruta, Appl Catal A-Gen. 369 (2009) 8-14.
[39] A. T. Bell, Science. 299 (2003) 1688-1691.
[40] C. Della Pina, E. Falletta, M. Rossi, Chem. Soc. Rev. 41 (2012) 350-369.
[41] Y. Liu, G. Zhao, D. Wang, Y. Li, Natl Sci Rev. 2 (2015) 150-166.
[42] T. Mallat,A. Baiker, Catal. Today. 19 (1994) 247-283.
[43] O. Špalek, J. Balej, I. Paseka, J. Chem. Soc., Faraday Trans.1. 78 (1982) 2349-2359.